The Cytoplasmic Filament System in Critical Point-dried Whole Mounts and Plastic-Embedded Sections

HANS RIS

Department of Zoology and High Voltage Electron Microscope Facility, University of Wisconsin, Madison, Wisconsin 53706

ABSTRACT High voltage electron microscopy of intact cells prepared by the critical point drying (CPD) procedure has become an important tool in the study of three-dimensional relationships between cytoplasmic organelles. It has been claimed that critical point-dried specimens reveal a structure that is not visible in sections of plastic-embedded material; it has also been claimed that this structure, in association with known cytoplasmic filaments, forms a meshwork of tapering threads ("microtrabecular lattice"). Alternatively, this structure might be a surface tension artifact produced during CPD. To test possible sources of artifacts during CPD, model fiber systems of known structure were used. It was found that traces of water or ethanol in the CO_2 caused distortions and fusion of fibers in pure muscle actin, fibrin, collagen, chromatin, and microtubules that produce a structure very similar to the proposed "microtrabecular lattice." These structures were, however, well preserved if water and ethanol were totally excluded from the CO_2. The same results were obtained with whole mounts of cultured cells. A "microtrabecular lattice" was obtained if some water or ethanol was present in the pressure chamber. On the other hand, when water or ethanol were totally excluded from the CO_2 during CPD, cytoplasmic filaments were uniform in thickness similar to their appearance in sections of plastic-embedded cells. It is concluded that the "microtrabecular lattice" is a distorted image of the cytoplasmic filament network produced during CPD by traces of water or ethanol in the CO_2.

The cytoplasm of most cells contains a complex and dynamic system of filaments which appear to determine many of its properties such as viscosity, elasticity, intracellular transport, cell shape, and motility. Microtubules (MT),[1] intermediate filaments (IF), and actin filaments are the major components that are becoming well characterized at the molecular level. In addition, thinner filaments (2–3 nm) of unknown chemical composition have been observed in many cells, usually as bridges connecting other filaments (9). The detergent-resistant filament complex has become known as the cytoskeleton. The usual ultrathin sections required for 100 kV electron microscopes provide relatively little information on the complex three-dimensional relationship between cytoplasmic filaments. High voltage electron microscopy (HVEM) resolves these filaments in much thicker preparations and has become the method of choice in such studies. Especially informative are stereoscopic micrographs of unsectioned intact cells (whole mounts) that can be grown directly on formvar-coated gold grids (see Fig. 1). To avoid surface tension artifacts during drying, such whole mounts are prepared with the critical point drying (CPD) procedure first used by Anderson (1).

In the last few years, a number of studies using this technique have appeared; these studies describe a new structural system thought to represent a matrix or "ground substance" that pervades all of the cell, and connects all organelles into an integrated "cytoplast." Called the "microtrabecular lattice" because of the resemblance to spongy bone, this structure is described as a network of tapering filaments which vary in thickness from 10 nm, where they contact other filaments or membranes, to 2 nm in their middle (11, 12). This structure

[1] *Abbreviations used in this paper*: CPD, critical point drying; HVEM, high voltage electron microscopy; IF, intermediate filaments; MT, microtubules.

THE JOURNAL OF CELL BIOLOGY · VOLUME 100 MAY 1985 1474–1487
© The Rockefeller University Press · 0021-9525/85/05/1474/14 $1.00

is not seen in sections of plastic-embedded cells where all filaments are of uniform thickness along their length. The "trabecular" structure however becomes visible in sections if the embedding matrix is extracted and the sections dried with CPD (13). This disparity has been explained by assuming that the microtrabeculae produce little contrast in plastic-embedded sections.

Various observations on critical point–dried whole mounts of relatively simple and well-characterized structures such as chromatin fibers suggested another explanation: the microtrabecular image may be produced by surface tension distortions of the filamentous cytoskeleton arising during CPD. It was noted, for instance, that chromatin fibers dried from amyl acetate or by CPD on humid days formed a meshwork of tapering filaments instead of the expected uniform 10-nm fibers (8). A similar effect was observed by Bahr and Engler (2) on critical point–dried chromosomes. Incomplete removal of water during CPD caused fusion and distortion of the chromatin fibers, thus producing a network of tapering or smudged fibers resembling "microtrabeculae" instead of the well-known 25-nm fibers of inactive chromatin. In addition, CPD whole mounts of cultured cells showed considerable variation from one preparation to another, from meshworks of uniform filaments to more or less pronounced trabecular or coarse alveolar structures. This study reports on a systematic analysis of the CPD procedure using as models several systems of biological fibers of known structure as well as various types of cultured cells to determine the possible distortions that can arise during CPD and how to avoid them. I conclude that the structural appearance called the "microtrabecular lattice" represents a characteristic distortion of nuclear and cytoplasmic filaments and associated components due to residual water or ethanol in the CO_2.

MATERIALS AND METHODS

Model Fibers

Purified rabbit skeletal muscle actin was obtained from Dr. Marion Greaser (Meat and Animal Science, University of Wisconsin at Madison). Formvar-carbon–coated grids were made hydrophilic by glow discharge and floated on a drop of actin solution on parafilm for 5 min. The grids were then floated on fixative (1% glutaraldehyde, 50 mM KCl, 50 mM sodium phosphate buffer [pH 7.0], 5 mM $MgCl_2$, 4% tannic acid [reference 4]) for 5 min, rinsed in H_2O, stained in 1% uranyl acetate for 10 min, dehydrated in ethanol or acetone, and critical point–dried with CO_2. In some cases amyl acetate was used as intermediate between ethanol and CO_2.

Rat skin collagen (obtained from Dr. Hynda Kleinmann, National Institutes of Health) was applied to formvar-carbon–coated grids, fixed in 2.5% glutaraldehyde in 1 mM PIPES buffer (pH 7.0), postfixed in 0.05% OsO_4, stained in 1% uranyl acetate, dehydrated in acetone, and critical point–dried. Mouse tail collagen was prepared by dispersing tail tendon suspended in Ringer's solution with a blender. The suspension was placed on formvar-carbon–coated grids, fixed in 2.5% glutaraldehyde in 0.1 M HEPES buffer (pH 7.0), stained in 1% uranyl acetate, dehydrated in ethanol, and critical point–dried.

Fibrin clots polymerized on formvar-carbon–coated grids made hydrophilic by glow discharge were obtained from Drs. M. Mueller and J. Ferry (Department of Chemistry, University of Wisconsin at Madison). The clots were fixed in 2.5% glutaraldehyde in 0.1 M HEPES buffer (pH 7.0), stained in 1% uranyl acetate, dehydrated in ethanol, and critical point–dried.

25-nm chromatin fibers were prepared by spreading erythrocytes from the frog *Rana pipiens* on a clean water surface. The surface layer was picked up by touching a formvar-carbon–coated grid made hydrophilic by glow discharge to the surface. The grids were fixed in 2.5% glutaraldehyde in 0.1 M PIPES buffer (pH 7.0), stained in 1% uranyl acetate, dehydrated in ethanol, and critical point–dried.

Microtubules from the peripheral band of frog erythrocytes were present in the same preparations as the chromatin fibers described above.

Whole Mounts and Thick Sections of Cells

Human skin fibroblast cultures were obtained from Dr. R. DeMars (Genetics Department, University of Wisconsin at Madison). The African green monkey kidney cell line (BSC-1), the baby hamster kidney (BHK-21) cell line, and the rat kangaroo kidney (PtK-1) cell line were originally purchased from American Type Culture Collection (Rockville, MD).

Coelomocytes from *Strongylocentrotus purpuratus* were isolated and purified according to the procedure of Otto et al. (6). Cells in the petaloid form were placed on formvar-carbon–coated gold grids on a slide, covered with a cover glass and monitored by phase-contrast microscopy. As the cells began to attach and transform into the filopod form, the coverslips were removed and the grids immersed in fixative.

FIXATION

Several different fixation schedules were used for both whole mounts and thick sections of cells.

WITHOUT TANNIC ACID: (*a*) 2% glutaraldehyde in 0.1 M PIPES (or HEPES) buffer (pH 7.0) 30 min, followed by either 0.05%, 0.1%, or 1% OsO_4 for 10 min; (*b*) same fixation without OsO_4; (*c*) 2% paraformaldehyde, 1.25% glutaraldehyde in 0.1 M phosphate buffer (30 min) followed by 1% OsO_4 for 30 min; (*d*) 2% glutaraldehyde in 0.1 M phosphate buffer (pH 7.0) for 10 min; or (*e*) 2% glutaraldehyde in 0.1 M HEPES buffer (pH 7.0) containing 0.05% saponin for 30 min.

WITH TANNIC ACID: (The first two procedures [a and b] [4, 5] were used to make the cell membrane permeable to tannic acid). (*a*) Exposure of cells to OsO_4 vapor for 5 s, followed by immersion in 2% glutaraldehyde in 0.1 M HEPES buffer (pH 7.0) containing either 0.2% or 2% tannic acid for 30 min followed with 0.05% or 0.1% OsO_4 for 10 min; (*b*) 2% glutaraldehyde in 0.1 M HEPES buffer (pH 7.0) containing 0.05% saponin and 0.2% tannic acid for 30 min followed by 0.1% OsO_4 for 10 min; or (*c*) 1% glutaraldehyde, 50 mM KCl, 50 mM sodium phosphate buffer (pH 7.0), 5 mM $MgCl_2$, 4% tannic acid (4).

CPD

This method was designed for drying specimens free of surface tension artifacts (1). Water is removed with ethanol or acetone and these in turn by thorough flushing with liquid CO_2 under pressure. The transition from liquid to gas by raising the temperature beyond the critical point avoids that any liquid-gas interface passes through the specimen. Experience has shown that even small traces of water or ethanol remaining in the CO_2 can cause distortion of biological structures. We have found that the following steps are required to remove all water and ethanol from the CO_2 in the pressure chamber: (*a*) Molecular sieve must be added to the absolute ethanol to make it free of water; (*b*) a water-absorbing filter must be attached to the CO_2 tank (for instance, the Tousimis filter #8782) (Tousimis Research Corp., Rockville, MD); (*c*) grid holders tend to trap residual ethanol which is not removed by simply passing liquid CO_2 through the pressure chamber. It is necessary to agitate the grid holder while replacing the CO_2. Using a Tousimis pvt-3 samdri, the procedure is as follows: Open tank value; open inlet and outlet valves. When liquid CO_2 flows into pressure chamber, close inlet valve. Warm pressure chamber to room temperature before removing pressure chamber cover to avoid condensation of water on chamber walls. Close outlet valve. Fill one half of the pressure chamber with water-free ethanol or acetone, add grid holder, and close pressure chamber. Cool the pressure chamber to ~15°C by placing dry ice on its cover or, where available, by any independent cooling of the chamber. Open inlet valve and fill the chamber, agitate the grid holder by shaking the drier box. Empty chamber to above the grid level and repeat the procedure ten times. Fill the chamber with CO_2 and leave for 10 min. Replace the CO_2 in the chamber another five times. Turn on the heater and after the chamber has reached ~43°C, release the gas slowly. The grids should be stored immediately in a desiccator that contains phosphorous pentoxide.

PREPARATION OF THICK SECTIONS

For 0.25-μm-thick sections, the plastic was prepared somewhat softer than for ultrathin sections (Epon-Araldite mixture of Mollenhauer). Diamond knives were used for sections up to 0.25 μm thick, the glass knives for thicker sections. The movement of the block was set at the slowest possible speed on the Sorvall MT2 microtome (DuPont Co., Wilmington, DE). Expansion of the sections was accomplished by xylene vapor. The ribbons were picked up from below by a copper wire loop covered with a 0.5% formvar film and lowered with proper orientation on a single hole (1 × 2 mm) grid sitting on a 3-mm peg.

Staining

Whole mounts were stained in 1% uranyl acetate for 10 min before dehydration. Thick sections were stained with 7.5% uranyl magnesium acetate in H_2O for 2 h at 50°C followed by Reynold's lead citrate for 20 min. To assure penetration of the stain into thick sections from both surfaces the sections were mounted on 0.5% formvar films only. After staining a thin layer of carbon was evaporated over the grid surface not carrying the sections.

Electron Microscopy

The preparations were photographed with the AEI EM-7 high voltage electron microscope at the Madison HVEM Facility, operated at 1,000 kV. Stereo micrographs were taken with the eucentric tilt stage at the tilt angles indicated in the figure legends.

RESULTS

Model Fiber Systems

To assess the effect on structure of certain parameters in CPD, I used several purified biological fibers whose structure is well known: skeletal muscle actin, microtubules, collagen, fibrin, and 25-nm chromatin fibers.

The parameters investigated were fixation, dehydrating agent, intermediate fluid, and the presence of residual water or intermediate fluid in the CO_2. Good preservation of structure was obtained with aldehydes alone or followed by OsO_4 in any of the usual buffers. Dehydration in ethanol or acetone gave identical results. Originally, amyl acetate was used between ethanol and CO_2, but direct mixing of ethanol or acetone with liquid CO_2 gave equally good preservation of structure. However, the presence of small amounts of water, ethanol, or acetone in the CO_2 during CPD caused characteristic distortions, probably due to surface tension effects. Water in the CO_2 may be due to incomplete dehydration (residual water in the "absolute" ethanol) or to water in the CO_2 tank. Molecular sieve can be used to remove water from commercial absolute ethanol and a filter is available to remove it from the CO_2 (see Materials and Methods). Complete purging of ethanol or acetone from the pressure chamber is essential, but may be impeded by the grid holder than can trap ethanol. Continuous flushing of CO_2 through the chamber does not prevent distortions. With the Tousimis pvt-3 samdri critical point drier and grid holder (#8761) we found it necessary to empty and refill the chamber at least 10 times with shaking of the entire apparatus during each refill for efficient mixing in order to remove all ethanol and avoid distortion of the structures.

Distortion of Structure Caused by Residual Water in the CO_2

WATER IN THE CO_2 TANK: By accident, a tank was obtained that contained demonstrable water after it was opened. It was used to prepare actin and collagen by CPD. Fig. 2 is a stereomicrograph of a dense area of actin filaments after CPD with water in the CO_2. The filaments have irregular width and appear fused into an alveolar network of tapering filaments. In contrast, Fig. 3 shows the same actin preparation after CPD without water or ethanol in the CO_2. Now the filaments are of uniform thickness (~10 nm with tannic acid in the fixative), and no lateral fusion occurs. In Fig. 4, a less dense area of actin fibers is shown after CPD with residual water in the CO_2. Again, the fibers vary in thickness and form a network resembling a "microtrabecular lattice." The distortion of the fibers is especially obvious where they touch the formvar film. Similar results were obtained with collagen. With water in the CO_2, the fibers appeared distorted and tended to fuse. The characteristic banding pattern of collagen was not preserved (Fig. 5). When water and ethanol were removed from the CO_2, the collagen fibers were uniformly thick and showed the typical banding pattern (Fig. 6).

INCOMPLETE ETHANOL DEHYDRATION: In a different series of experiments, MT and 25-nm chromatin fibers were transferred from 95% ethanol into CO_2. This also leaves some water in the preparation during CPD. The results are shown in Fig. 7 for MT and Fig. 10 for chromatin fibers. Again we see distortion of the fibers. MT are more resistant than chromatin, which forms a network of fused fibers of uneven thickness. Well-dried MT and chromatin are seen in Figs. 9 and 12.

Distortion of Structure Caused by Residual Ethanol in the CO_2

The presence of residual ethanol in the CO_2 causes the same kinds of distortions as residual water; fibers are unevently thick and form networks of tapering filaments. This is shown for MT in Fig. 8, for chromatin in Fig. 11, and for fibrin in Fig. 13. They should be compared with the well-dried structures in Figs. 9, 12, and 14, respectively.

These experiments with biological fibers of known composition and structure have demonstrated that the presence of residual water or ethanol in the CO_2 during CPD causes characteristic distortions. The fibers are unevenly broadened and tend to fuse into networks of tapering filaments. The distortion is more pronounced at higher concentrations of filaments when they are in close proximity, or when they are near surfaces such as support films. In other words, a network of fused tapering filaments can be induced during CPD from populations of uniformly thick filaments including actin, collagen, microtubules, fibrin, and chromatin. These results emphasize the need for caution in interpreting cytoplasmic structure after CPD, and the importance of removing all traces of water and ethanol from the specimen before heating the CO_2 during CPD.

Whole Mounts of Intact Cells

The experiments with pure fiber systems raised the possibility that the "microtrabecular lattice," rather than representing a new organelle, is an artifact produced during CPD by distortion of the various cytoplasmic fibers. Experiments with mammalian cultured cells and coelomocytes from sea urchins were carried out to test whether cytoplasmic fibers are of uniform thickness in whole mounts as they are in sections of plastic-embedded cells if water and ethanol are removed from the CO_2 before CPD. We also investigated the effect of tannic acid in the fixative on the appearance of cytoplasmic filaments after CPD.

Fig. 15 illustrates a thin area of a BSC-1 cultured cell prepared by CPD. MT are smooth with a less dense center. Vesicles of various sizes appear enmeshed in a complex network of filaments. These filaments have uniform thickness, mostly ~6–7 nm. Some thinner connecting filaments are also visible. Particles ~10 nm in diameter are conspicuous along most of the filaments (arrow). Fig. 17 shows a similar thin area of a PtK-1 cell. The structure is similar; vesicles and polysomes are enmeshed in a complex system of longer and shorter filaments. All filaments are uniform in thickness. A

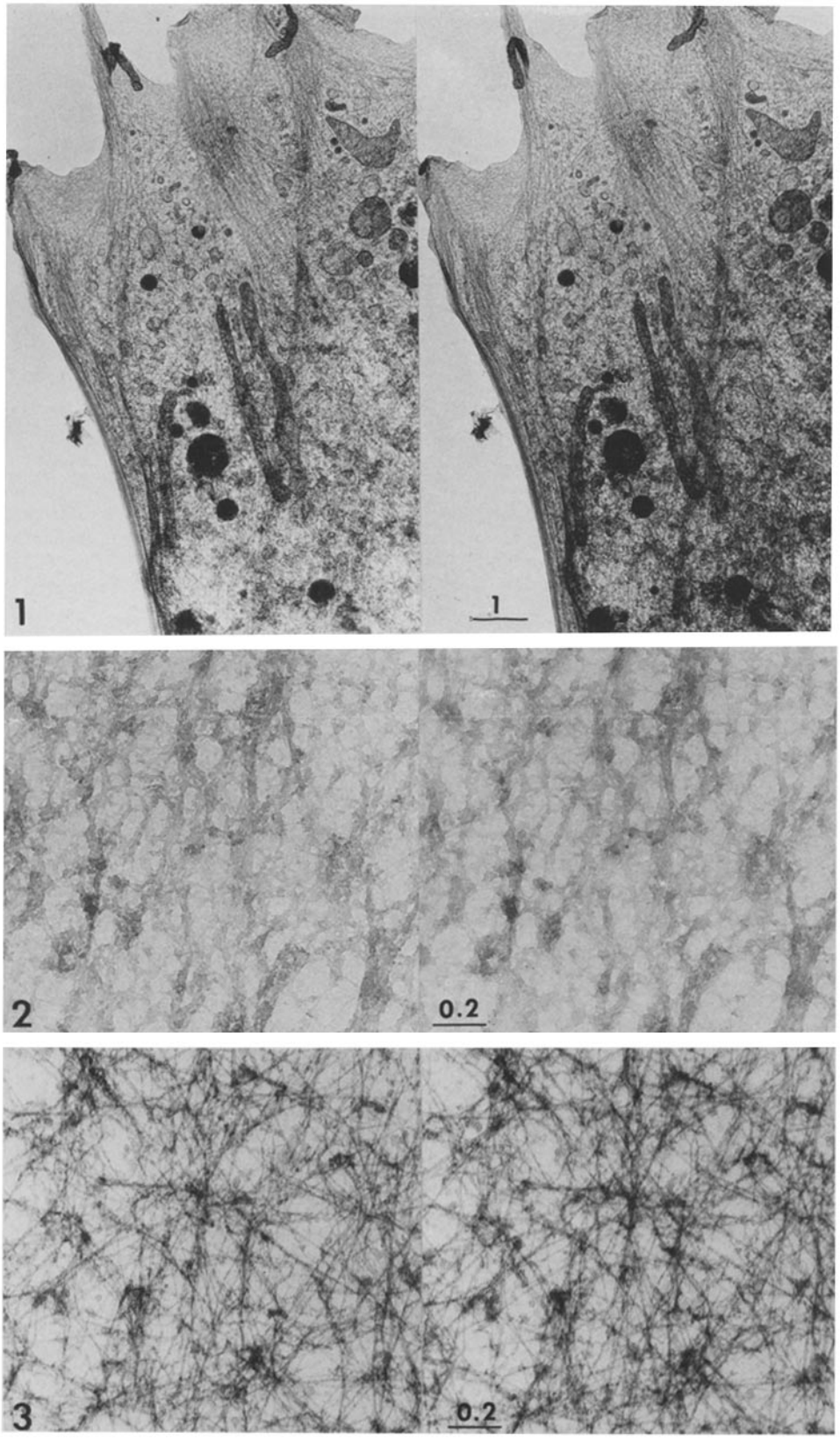

FIGURES 1–3 (Fig. 1) Human skin fibroblast grown on gold grid. Fixation schedule as in WITHOUT TANNIC ACID (C) (glut-phosph. buffer; 1% OSO_4) followed by dehydration in acetone, and CPD. This photograph illustrates the advantage of relatively low magnification stereomicrographs of intact cells for studies of interrelationships of cytoplasmic organelles. This and the following stereomicrographs should be viewed with a 2x magnifying stereo pocket viewer. Tilt angle 20°. × 7,500. (Fig. 2) Rabbit skeletal muscle actin solution on formvar-carbon-coated grid. Fixation schedule as in WITH TANNIC ACID (C), followed by dehydration in acetone, and CPD with CO_2 that contained water. Actin filaments are irregularly swollen and fused into alveolar networks. Tilt angle 10°. × 40,000. (Fig. 3) Rabbit skeletal muscle actin solution on formvar-carbon-coated grid. Same fixation as Fig. 2, followed by dehydration in ethanol, and CPD with dry CO_2. Actin filaments are distinct and uniform in thickness. Tilt angle 7°. × 40,000.

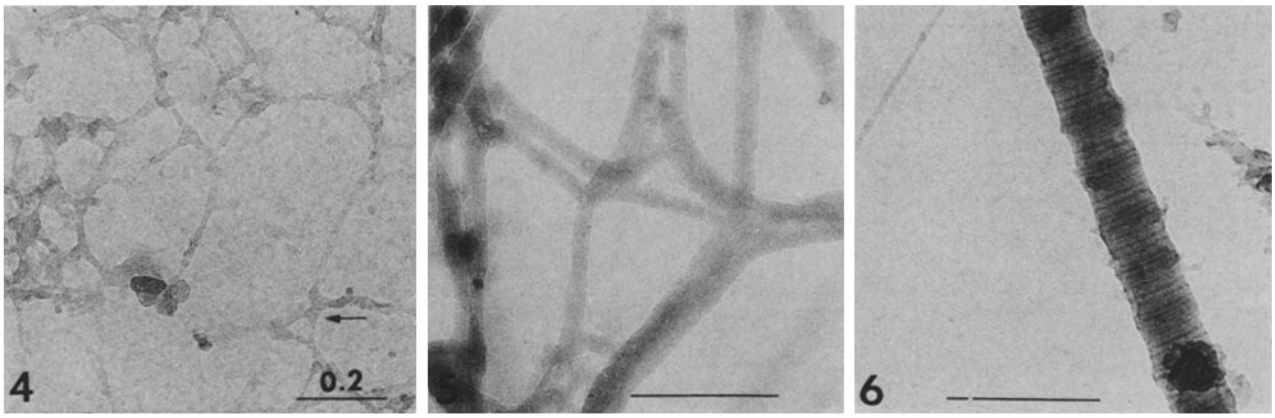

FIGURES 4–6 (Fig. 4) Rabbit skeletal muscle actin, lower concentration than in Fig. 2. Fixation schedule as in WITHOUT TANNIC ACID (*d*) (glut-phosp. buffer), followed by staining with 1% uranylacetate, dehydration in acetone, and CPD with water in CO_2. Individual filaments are visible. They vary in thickness along their length and broaden especially where they fuse with other filaments or contact the supporting film (arrow). × 60,000. (Fig. 5) Rat skin collagen. Fixation schedule as in WITHOUT TANNIC ACID (*a*) (glut-PIPES; 0.05% OsO_4), followed by staining with 1% uranylacetate, acetone dehydration, and CPD without water filter on CO_2 tank. The collagen banding is not preserved. × 100,000. (Fig. 6) Collagen from mouse tail tendon. Fixation schedule as in WITHOUT TANNIC ACID (*b*) (glut-HEPES) followed by staining with 1% uranylacetate, ethanol dehydration, and CPD with water filter on CO_2 tank. The cross-banding is preserved with a repeat of ~650Å. × 100,000.

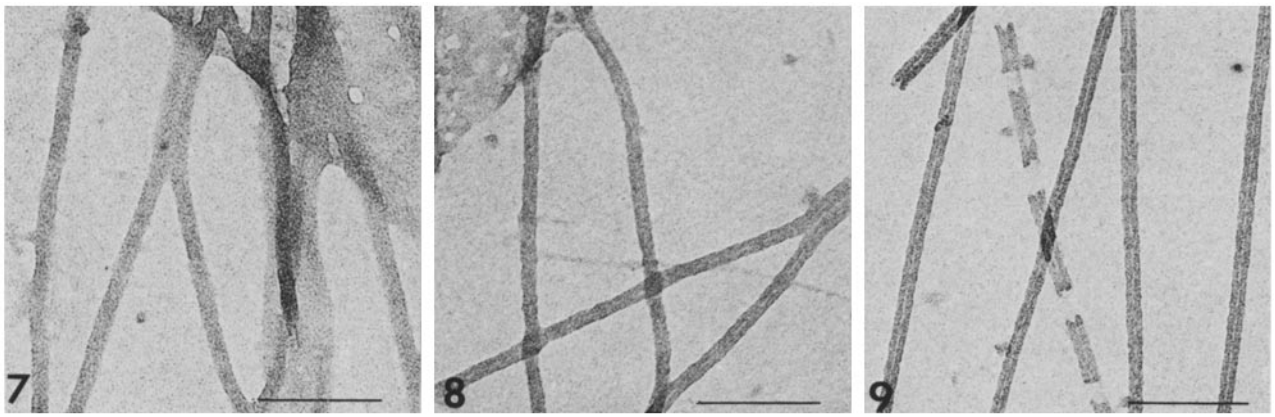

FIGURES 7–9 (Fig. 7) Microtubules (MT) from the peripheral band of frog erythrocytes. Fixation schedules as in WITHOUT TANNIC ACID (*b*) (glut-PIPES), followed by staining with 1% uranylacetate, incomplete ethanol dehydration into liquid CO_2 from 95% ethanol, and CPD. With water present, the MT have a fuzzy outline, they tend to fuse, and the tubular structure is not preserved. × 80,000. (Fig. 8) MT prepared and fixed as in Fig. 7, followed by complete dehydration but with ethanol not totally removed by CO_2. After CPD, MT tend to fuse and the lumen appears mostly obliterated. × 80,000. (Fig. 9) MT prepared and fixed as in Fig. 7, followed by complete dehydration and with ethanol fully removed by CO_2. After CPD, in the absence of water and ethanol, the MT appear crisp with the lumen well preserved. × 80,000.

whole mount of a BHK-21 cell prepared by CPD is shown in Fig. 27. The actin filaments of stress fibers are individually discrete and uniformly thick as they appear in sections. Mitochondria show characteristic cristae and dense matrix.

In contrast, cytoplasmic filaments look very different if traces of water are left in the CO_2. Fig. 18 shows a thin area of cytoplasm in a CPD whole mount of a PtK-1 cell prepared without the water-absorbing filter on the CO_2 tank. MT have uneven outlines and do not show the tubular appearance. Microfilaments are unevenly thick and tend to fuse into alveolar networks as observed with pure actin that was dried with water in the CO_2 (Figs. 2 and 4). Fig. 18 should be compared with Fig. 17, a PtK-1 cell treated identically except that the water-absorbing filter was present during CPD. In Fig. 24, the thin lamella at the edge of a PtK-1 cell is seen, again prepared without the water-absorbing filter. A coarse network of tapering filaments is the only structure visible here (compare this with Fig. 22, which represents a well-dried lamella). The appearance of IF after CPD without the water-absorbing filter is shown in Fig. 19. Individual filaments are not visible; instead we find an alveolar network of tapering filaments.

Identical networks of fused tapering filaments are observed in whole mounts of cells if ethanol is not completely removed from the CO_2 before CPD (not shown).

Maupin and Pollard (4) demonstrated that tannic acid protects actin filaments against fragmentation by OsO_4. I therefore investigated the effect of tannic acid on the appearance of cytoplasmic filaments in whole mounts. To make cells permeable to tannic acid, they were briefly exposed to OsO_4 vapor before immersion into the tannic acid-containing fixative (4), or saponin was added to the fixative (5).

Fig. 20 shows a PtK-1 cell fixed in the presence of tannic acid and prepared by CPD without filter on the CO_2 tank. In

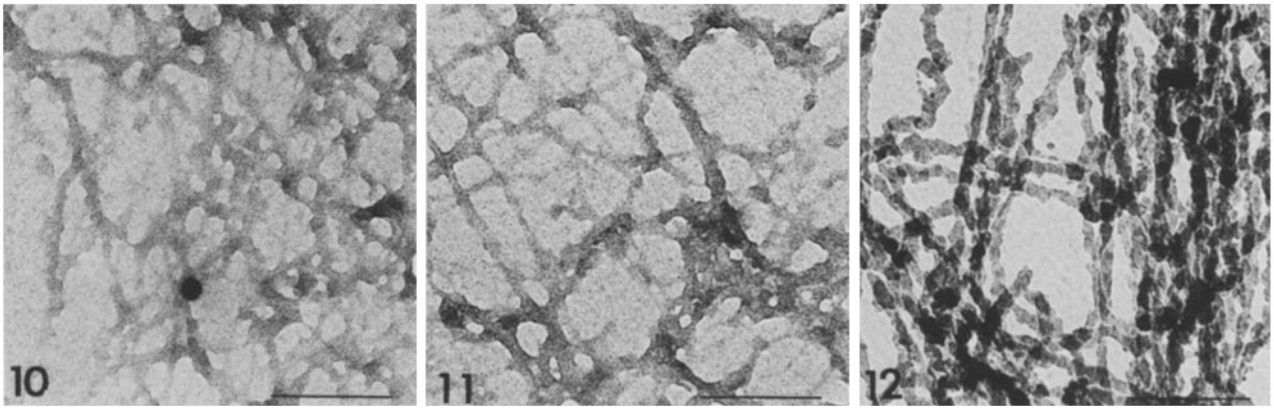

FIGURES 10–12 (Fig. 10) Frog erythrocyte chromatin, fixation schedule as in WITHOUT TANNIC ACID (*b*) (glut-PIPES), followed by staining with 1% uranylacetate, and incomplete dehydration, from 95% ethanol into CO_2. After CPD, the 25-nm chromatin fibers appear diffuse, vary in thickness, and are fused into an alveolar network. × 80,000. (Fig. 11) Frog erythrocyte chromatin prepared and fixed as in Fig. 10, followed by full dehydration in ethanol, but with ethanol not totally removed by CO_2. After CPD, with some ethanol present, the chromatin fibers vary in thickness, have diffuse outlines, and fuse into an alveolar network. × 80,000. (Fig. 12) Frog erythrocyte chromatin prepared and fixed as in Fig. 10, followed by full dehydration in ethanol, and with ethanol fully removed by CO_2. After CPD, the fibers have sharp outlines and do not fuse. × 80,000.

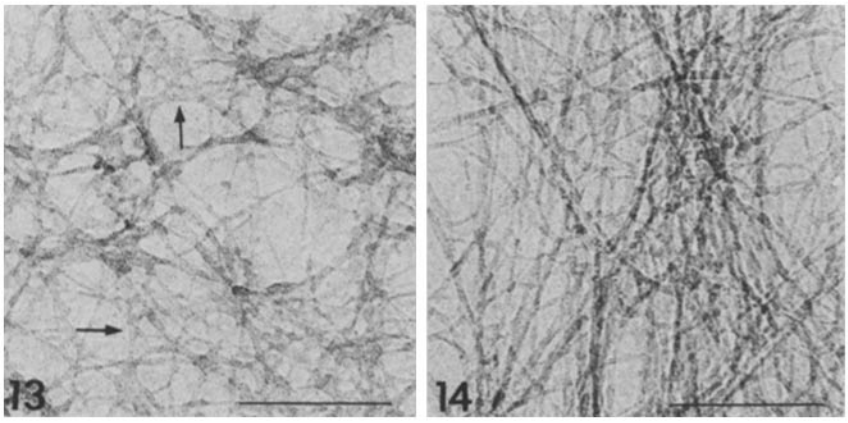

FIGURE 13 and 14 (Fig. 13) Bovine fibrin clot. Fixation schedule as in WITHOUT TANNIC ACID (*b*) (glut-HEPES), followed by staining with 1% uranylacetate, and ethanol dehydration but with ethanol not completely removed by CO_2. After CPD, the filaments are unevenly thick and tend to fuse. They are thicker at points of contact and taper away from them (arrows). × 100,000. (Fig. 14) Bovine fibrin clot. Fixation and staining as in Fig. 13, followed by ethanol dehydration, and with complete exchange of ethanol by CO_2. After CPD, fibers are uniform though they tend to align in groups. Stereo pictures show that in points of overlap, there is no real fusion of fibers. × 100,000.

contrast to Fig. 19, the IF are now distinct and the filaments have uniform width. The cell in Fig. 20 was actually prepared by CPD together with that of Fig. 19. Tannic acid thus protects the actin filaments from the surface tension distortion visible in Fig. 19. The distinctness of the microfilaments is not due to extraction of a "cytoplasmic ground substance" by the detergent (10) because the cell of Fig. 24, which shows a typical network of tapering filaments, was treated with saponin in the fixative but without tannic acid.

The structure of the thin lamella at the edge of the cell as it appears in tannic acid–fixed whole mounts is illustrated in Fig. 22. Three structures are present here: a network of 6–7-nm filaments, presumably actin, thinner connecting filaments (2–3 nm, short arrow), and particles of unknown composition ~10-nm in diameter attached to the filaments (long arrow).

Fig. 23 shows the spreading edge in a whole mount of a coelomyocyte from the sea urchin *S. purpuratus* fixed with tannic acid. The structure is very similar to the lamella in mammalian cells in culture. The predominant feature is a network of 6–7-nm filaments with attached particles. As in mammalian cells the mesh of the network is smallest just below the plasma membrane and the filaments are uniform in thickness.

The Cytoplasmic Filament System in Thick Sections

The advantage of whole mounts is of course the excellent contrast due to absence of embedding plastic, the possibility of seeing the entire cell and not just a very thin slice of it, and the ease in establishing the three-dimensional relationship between organelles especially in stereoscopic micrographs. However, because of the complexity of cytoplasmic organization and overlap of structures, the use of whole mounts is limited to cells that have regions no thicker than 0.5–1 μm, even when viewing them with a 1 MeV microscope. Such cells cannot be prepared as whole mounts and must be studied in sections after plastic embedding. It is therefore of interest to know what the cytoplasmic structures look like in thick sections especially in comparison with whole mounts of comparable thickness. Fig. 21 shows the thin lamella at the edge of a BSC-1 cell in a 0.5-μm-thick section. The major structural component here is an irregular network of filaments 6–7 nm thick, most likely composed of actin. Associated with these filaments are particles ~10 nm in diameter (long arrow). Occasionally one also sees thinner filaments (~3 nm thick) (short arrow). The filaments are uniform in thickness. A

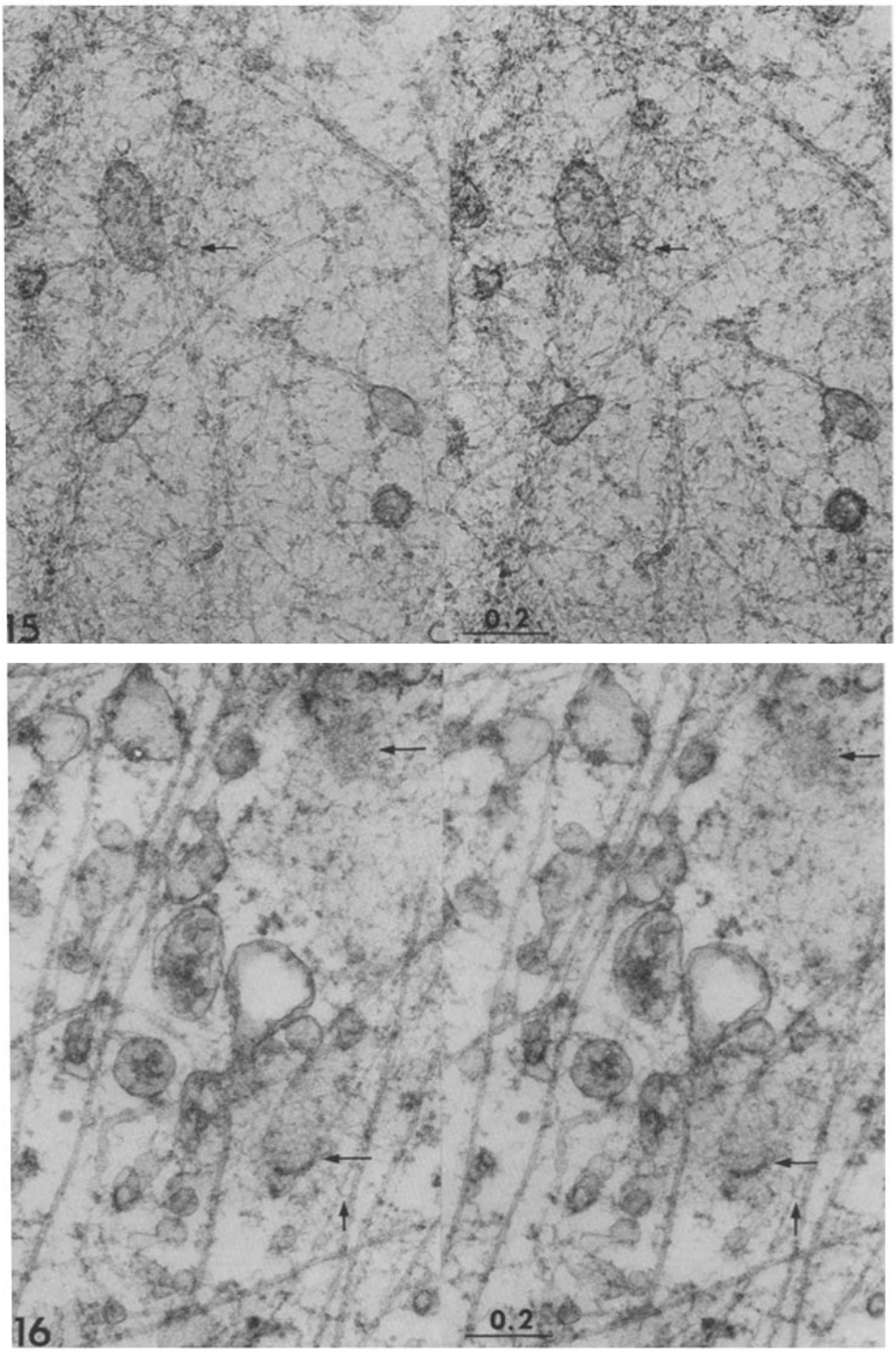

FIGURES 15 and 16 (Fig. 15) BSC-1 cell, whole mount. Fixation schedule as in WITHOUT TANNIC ACID (*a*) (glut-HEPES; 0.05% OsO_4), followed by staining with 1% uranylacetate, and ethanol dehydration. After CPD, the lumen in MT is well preserved. Filaments are uniformly thick and carry many particles ~10 nm thick along their length (arrow). The longer filaments are ~5 nm thick; many shorter ones are 2–3 nm. Tilt angle 10°. × 60,000. (Fig. 16) BSC-1 cell, section 0.25-μm-thick. Fixation as in Fig. 15 but with 1% OsO_4, followed by staining with 1% uranylacetate, and ethanol dehydration, Epon-Araldite. The right hand edge includes the cell surface with two coated pits (long arrows). The clathrin polygons and neighboring cytoskeletal elements are visible. IF show cross-connections to MT (short arrow). Tilt angle 10°. × 60,000.

coated pit is visible at the arrowhead. If one compares this image with the corresponding area in a whole mount (see Fig. 22), one notices that, except for higher contrast in whole mounts, the structure is very similar with uniformly thick filaments and attached particles.

This similarity of cytoplasmic structure in whole mounts and thick sections is further documented for a more central area of a PtK-1 cell in Figs. 25 and 26. Fig. 25 represents a 0.25-μm-thick section and Fig. 26 represents a CPD whole mount. In both preparations, the IF in the bundles are indi-

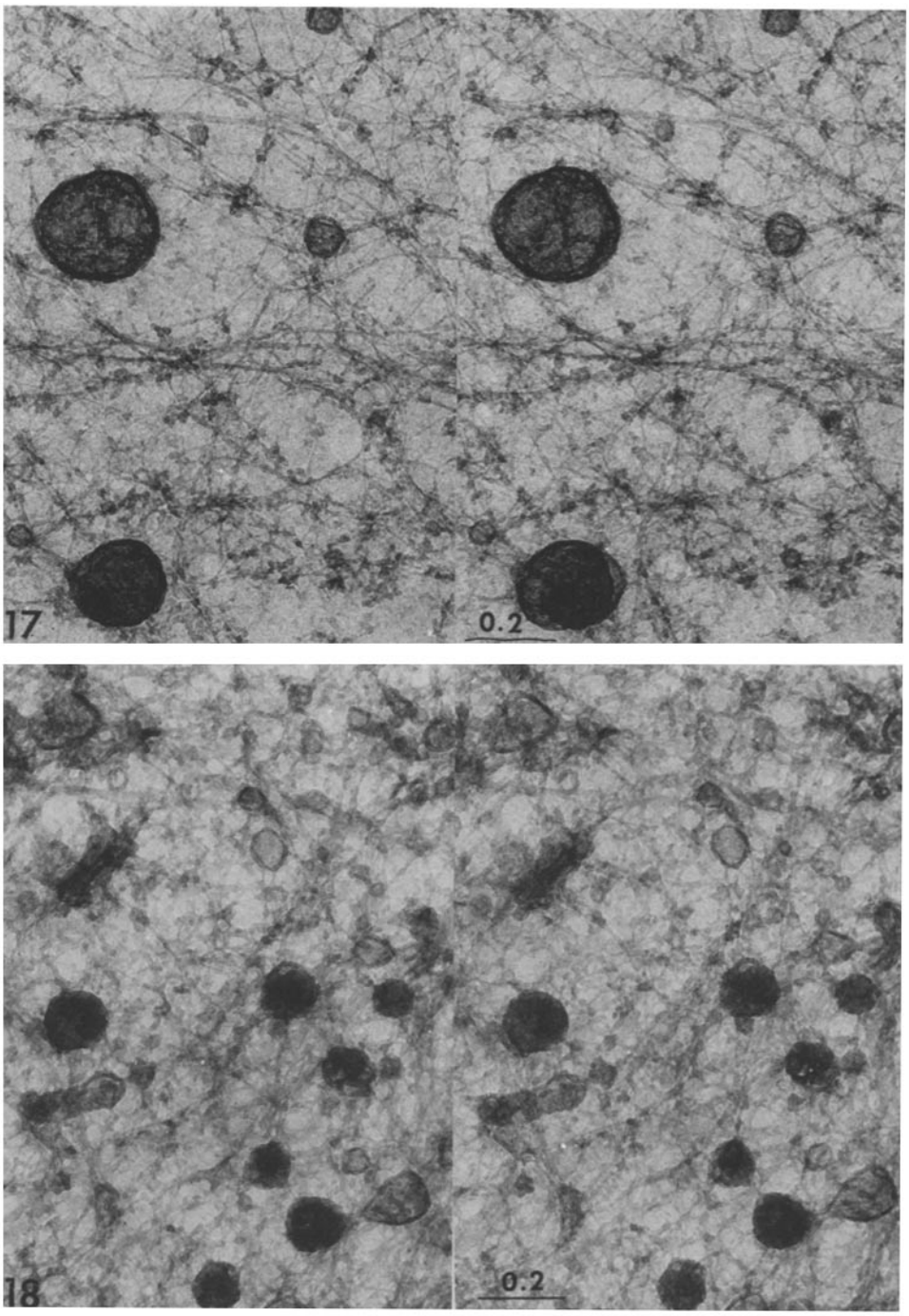

FIGURES 17 and 18 (Fig. 17) PtK-1 cell, whole mount. Fixation schedule as in WITHOUT TANNIC ACID (*b*) (glut-HEPES), followed by staining with 1% uranylacetate, and ethanol dehydration. After CPD with water filter on CO_2 tank, the filaments are uniform, mostly ~5 nm thick. In addition to ribosomes, one finds less opaque particles ~10 nm in diameter along the fibers. Tilt angle 10°. × 60,000. (Fig. 18) PtK-1 cell, whole mount. Fixation schedule as in Fig. 17, followed by staining with 1% uranylacetate, and ethanol dehydration as in Fig. 16, but critical point-dried without the filter on the CO_2 tank. The filaments show extensive fusion and are uneven in thickness. Particles are indistinct and appear to have fused onto the filaments. Compare with Fig. 17. Tilt angle 10°. × 60,000.

vidually distinct and uniformly thick. With proper staining, excellent contrast of cytoplasmic fibers is obtained even with thick sections photographed at 1 MeV. The following micrographs give some examples of cytoplasmic organization in cultured mammalian cells. Fig. 16 is a 0.25-μm-thick section near the surface of a BSC-1 cell. Two coated pits are visible (long arrows) showing the clathrin coat and surrounding filament net adjacent to the plasma membrane. Parallel MT and IF show thin side branches which often connect MT and IF (short arrow). Particles are seen associated with the actin net and with IF. Many of the vesicles appear connected to the cytoskeleton through thin filaments. A thicker area of a cell

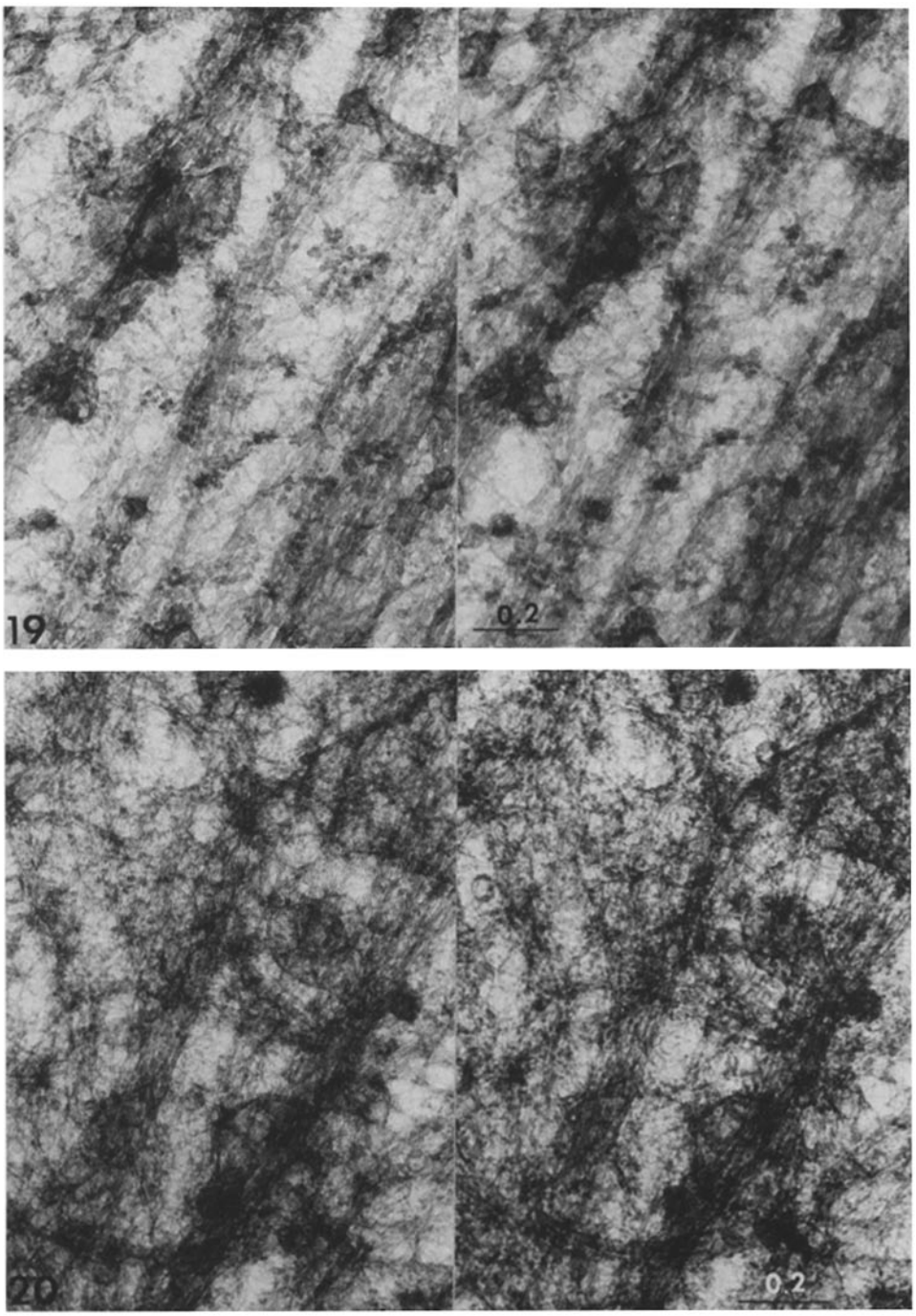

FIGURES 19 and 20 (Fig. 19) PtK-1 cell, whole mount. Fixation schedule as in WITHOUT TANNIC ACID (*a*) (glut-HEPES, 0.1% OsO_4), followed by staining with 1% uranylacetate. After CPD without water filter on CO_2 tank, several bundles of IF are visible here. The filaments show the uneven thickness and fusion obtained with water in the CO_2. Connecting the bundles are tapering filaments arranged in networks. Tilt angle 10°. × 60,000. (Fig. 20) PtK-1 cell, whole mount. Fixation schedule as in WITH TANNIC ACID (*b*) (glut-HEPES, saponin, tannic acid; 0.1% OsO_4), followed by staining with 1% uranylacetate, ethanol dehydration, and CPD without water filter on CO_2 tank. This cell was processed through CPD together with that of Fig. 19. Note that after tannic acid fixation the filaments in the IF bundles are distinct and uniform in thickness. It appears that the tannic acid decreases or prevents the distortion caused by traces of water in the CO_2. Tilt angle 10°. × 60,000.

is seen in Fig. 28. In this area we find a dense array of cytoskeletal elements oriented in parallel. 7-nm (actin) filaments are cross-connected in bundles or as networks. IF and MT are often parallel and connected at intervals by thin filaments. Small particles (~10 nm) are frequently attached to the filaments. Polysomes and small vesicles appear linked to the filaments.

The Organization of the Cytoplasm As Seen in CPD Whole Mounts and Thick Sections

One major conclusion of this study has already been mentioned: the cytoplasmic structure as seen in CPD whole mounts is basically the same as that seen in sections of similar cells embedded in plastic. We see the same elements: 7-nm

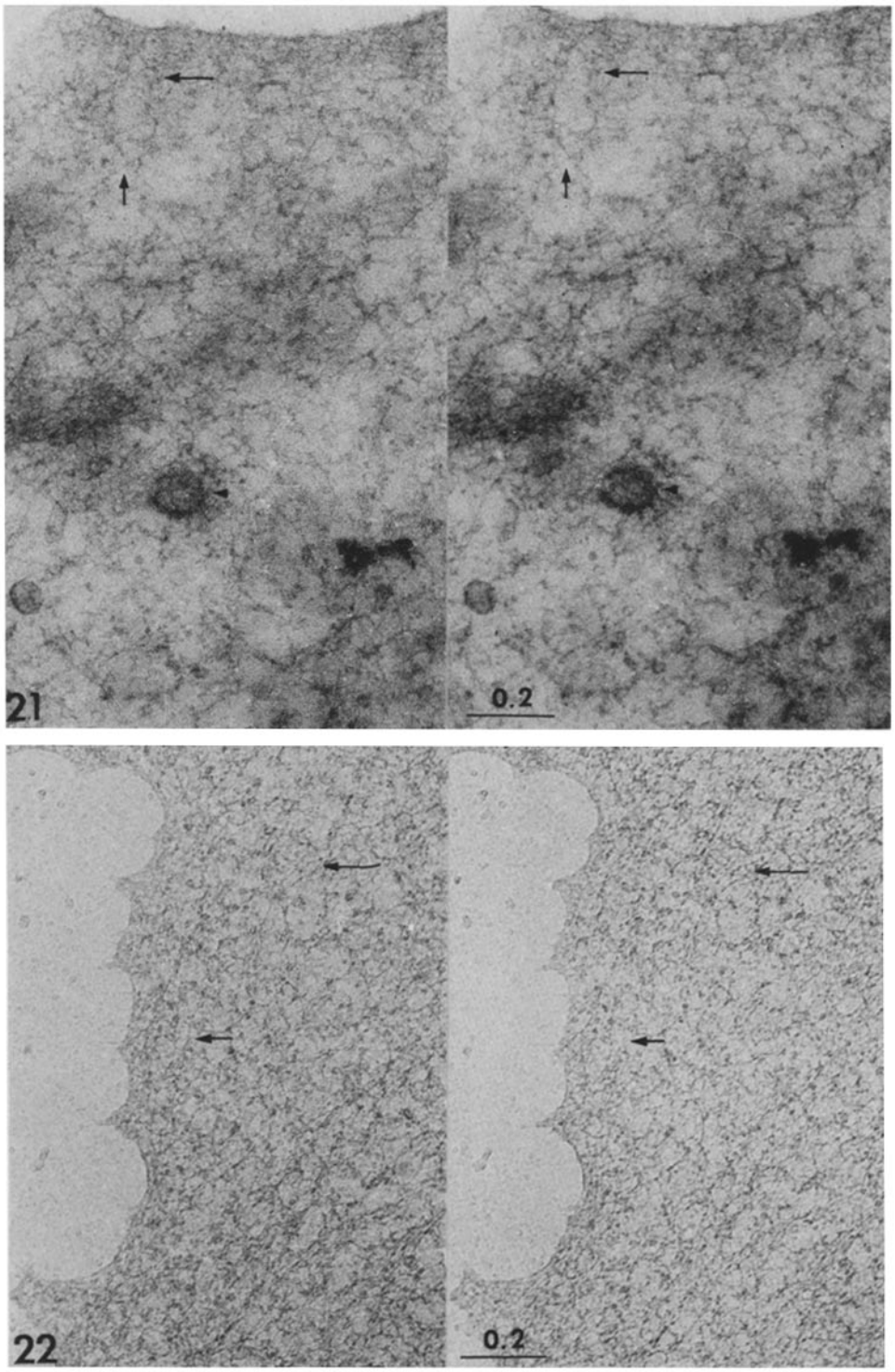

FIGURES 21 and 22 (Fig. 21) Cell margin of a BSC-1 cultured cell, 0.5-μm section of plastic-embedded cell. Fixation schedule as in WITHOUT TANNIC ACID (a) (glut-HEPES; 1% OsO_4). Stained with 1% uranylacetate, followed by ethanol dehydration, Epon-Araldite. The structure seen in this section is identical to that in the whole mount (Fig. 22): 6–7 nm filaments, 3-nm filaments (short arrow), and 10-nm particles (long arrow). The arrow head points to a coated pit. Tilt angle 10°. × 60,000. (Fig. 22) Cell margin of a BSC-1 cultured cell. Fixation schedule as in WITH TANNIC ACID (a) (OsO_4 vapor; glut-HEPES, tannic acid), followed by staining in 1% uranylacetate, ethanol dehydration, and CPD. The lamina at the cell edge contains a network of 6–7-nm filaments (presumably actin), 3-nm filaments (short arrows), and 10-nm particles (long arrows) attached to filaments. The filaments are uniform along their length. Tilt angle 10°. × 60,000.

microfilaments singly, in bundles, or as networks; IF singly or as bundles; MT; 2–3-nm cross-connections between these elements, and variable numbers of small particles (~10 nm) attached to all filament types. The relative abundance and patterns of association of these elements varies from one area of the cell to another and presumably undergoes temporal variation in relation to cell activity; but in every case the filaments are of uniform width and there is no sign of a

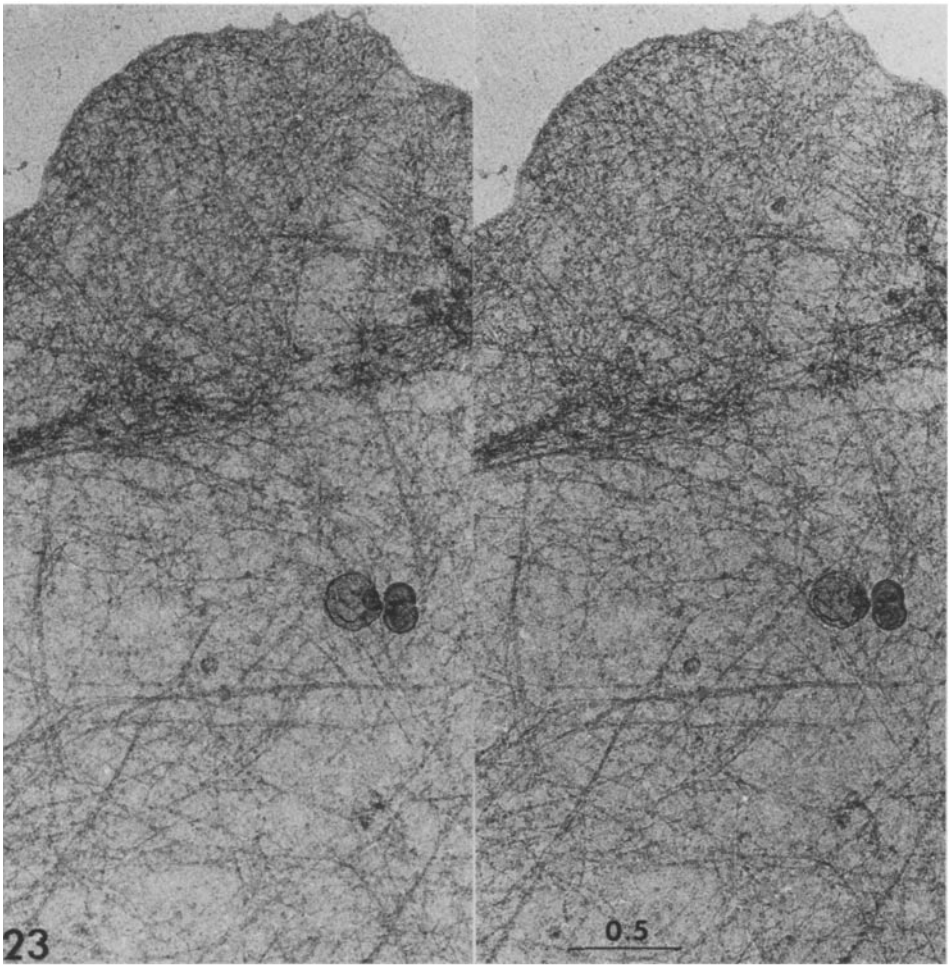

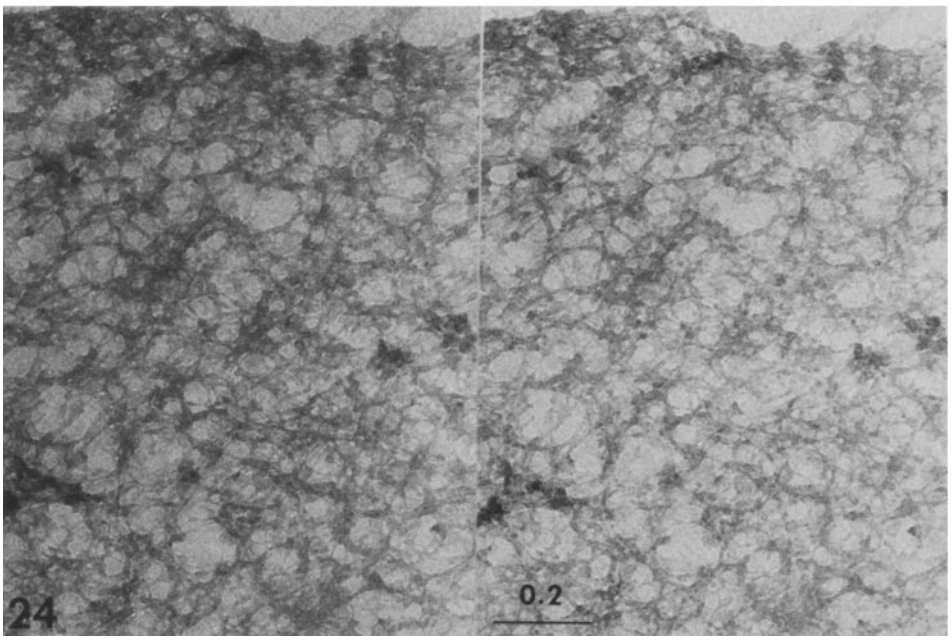

FIGURES 23 and 24 (Fig. 23) Coelomocyte of the sea urchin *S. purpuratus* after attachment to a formvar-coated grid. Whole mount. Fixation schedule as in WITH TANNIC ACID (*a*) (OsO_4 vapor; glut-phosphate buffer, 2% tannic acid; 1% OsO_4), followed by staining with 1% uranylacetate and ethanol dehydration. After CPD, the thin cell margin contains mainly 6–7-nm filaments with attached 10-nm particles. The filaments are uniform in thickness. Tilt angle 11°. × 30,000. (Fig. 24) PtK-1 cell, whole mount. Fixation schedule as in WITHOUT TANNIC ACID (*e*) (glut-HEPES, saponin), followed by staining with 1% uranylacetate, and ethanol dehydration. After CPD without water filter on CO_2 tank, this cell edge shows the typical distortion of filaments and filament fusion when traces of water are present in the CO_2. Note that the 10-nm particles seen on filaments in well-dried preparations and in sections (Figs. 22 and 23) are not preserved under these conditions. Tilt angle 10°. × 60,000.

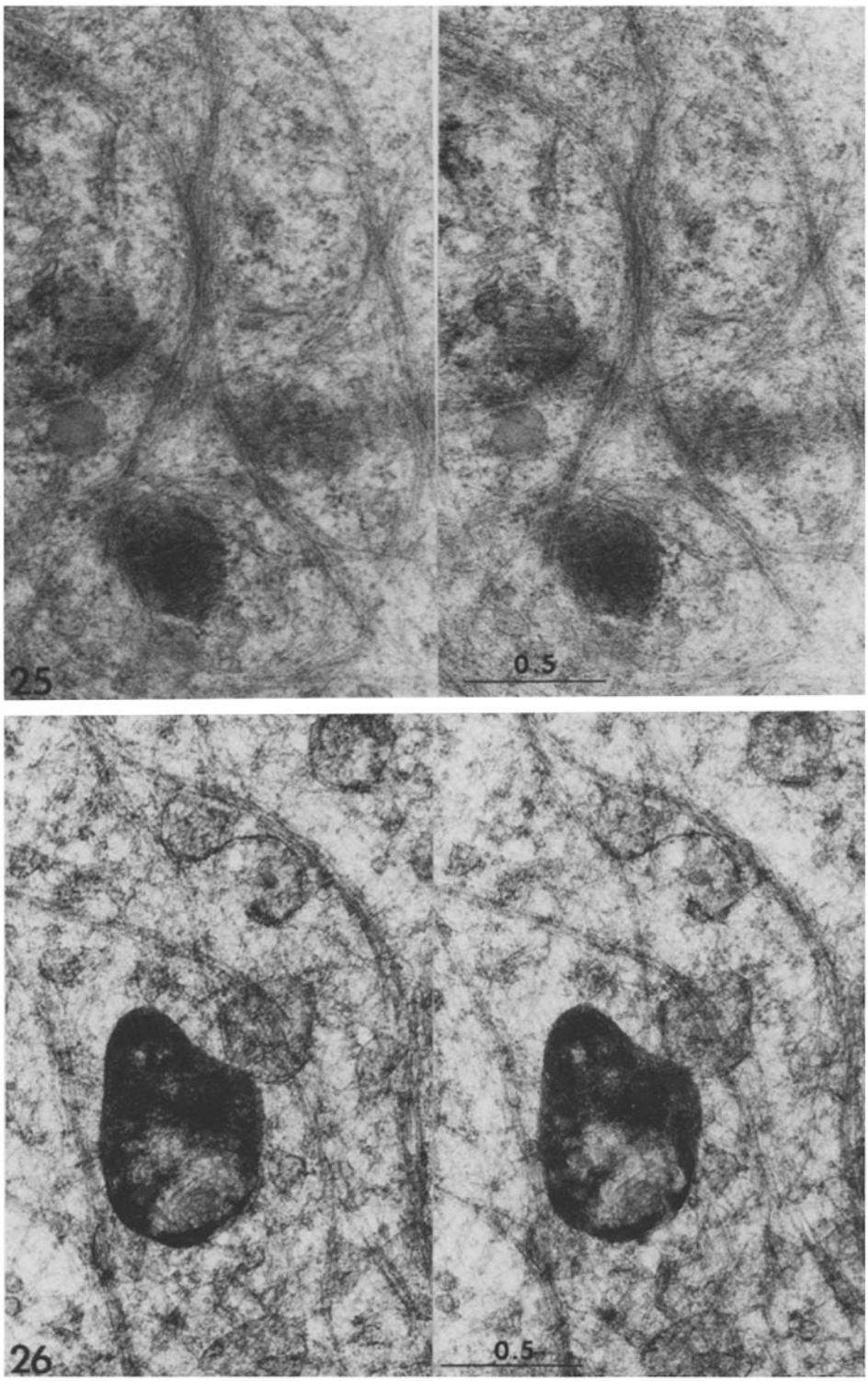

FIGURES 25 and 26 (Fig. 25) PtK-1 cell, area with bundles of IF. Section 0.25-μm-thick. Fixation as in Fig. 1, followed by staining with 1% uranylacetate, and ethanol dehydration, Epon Araldite. Tilt angle 10°. × 40,000. (Fig. 26) PtK-1 cell, whole mount. Fixation as in Fig. 20, followed by dehydration and CPD. Note that in this whole mount as in the section (Fig. 25), the IF are distinct and uniformly thick. Except for the greater contrast in the whole mount, the cytoplasmic structure in whole mounts and sections is identical. Tilt angle 10°. × 40,000.

separate, anastomotic network of tapered cross-linking elements. In other words, after optimal dehydration and CPD, whole mounts do not display the "microtrabecular" image that has been interpreted as indicating an additional, distinct, pervasive form of ordered ground substance.

DISCUSSION

The availability of million volt electron microscopes has made it possible to see intact cells grown on formvar-coated gold grids in stereo; this supplies information previously unavail-

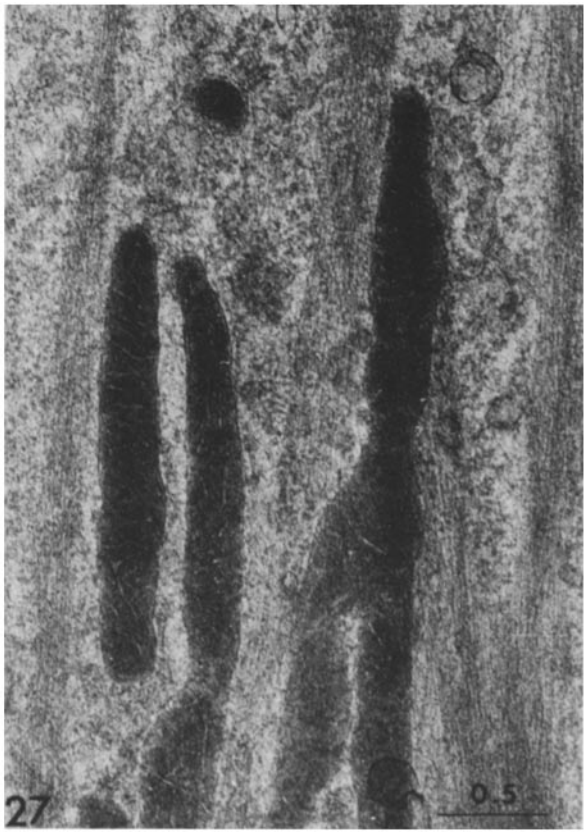

FIGURE 27 BHK-21 cell, whole mount. Fixation schedule as in WITH TANNIC ACID (a) (OsO_4 vapor; glut-phosph-buffer, 0.2% tannic acid; 0.05% OsO_4). Stained with 1% uranylacetate, followed by acetone dehydration and CPD. The filaments in the stress fibers are individually distinct and mitochondria show cristae and dense matrix as known from plastic-embedded sections. × 30,000.

able on three-dimensional relationships of cellular organelles. For electron microscopy, such whole mounts of cells or organelles have to be dried without surface tension distortions. This can be accomplished with the CPD procedure of Anderson (1).

In recent years, CPD has been used to study the cytoplasmic filament system in a variety of cultured cells. It led to the postulation of a new cell component described as a structured cytoplasmic ground substance called the "microtrabecular lattice" (3, 7, 11, 12). The anastomosing trabeculae in this lattice have a characteristic appearance: they are more than 10 nm thick where they join other fibers but often only 2–3 nm in their center. These trabeculae have been described as being continuous with cytoskeletal elements and as appearing to enmesh all cytoplasmic organelles. However, they are not visible in sections of plastic-embedded cells, a fact typically attributed to their low contrast relative to the embedding matrix. They are reported to be visible in thin-sectioned cells only when such cells are prepared by the polyethylene glycol embedding method (3, 13). Here the cells can be viewed after the resin has been extracted and the sections have been critical point–dried, as with whole mounts. Curiously, in such extracted material microtrabeculae are visible not only in the cytoplasm of nonmuscle cells, but also in place of the normal myofilament system in muscles, in the nucleus, and in such accessory structures as the axonemes of flagella, leading to the extraordinary claim that dynein arms and spokes and myosin cross-bridges are simply different forms of microtrabeculae. Since such a novel viewpoint is derived exclusively from critical point–dried material, it behooved me to determine whether or not CPD could generate certain characteristic artifacts.

The approach taken here was to study the effect of CPD on a variety of isolated "model fibers" whose structure was known from the use of independent techniques. According to such criteria, muscle actin, chromatin, fibrin, collagen, and microtubules are well preserved by CPD if an effort is made to exclude water and ethanol from CO_2. The characteristic banding of collagen, for instance, is well conserved. On the other hand, traces of water or ethanol in the CO_2 result in distortion and fusion of fibers and destroy the banding in collagen and the tubular appearance of microtubules.

These networks of distorted actin, fibrin, and chromatin filaments strongly resemble the "microtrabecular lattice" illustrated in the studies from Porter's laboratory (7). Therefore the thick-thin tapering filaments and alveolar networks of the "microtrabecular lattice" could be distortions produced during CPD. Indeed, in cell whole mounts prepared with all precautions to exclude water or ethanol from the CO_2, the cytoplasmic filaments are uniformly thick and not tapering. Frequently, 10-nm particles of unknown nature are attached to cytoplasmic filaments. If traces of water or ethanol are introduced into the CO_2 on purpose by incomplete dehydration of the sample, by omission of the water-absorbent filter on the CO_2 tank, or by incomplete replacement of ethanol by CO_2 in the pressure chamber, then a characteristic "microtrabecular lattice" appears in all cells that have been studied.

Hence cytoplasmic filaments in situ are subject to the same distortions as observed with isolated filaments. In addition, we find that in distorted samples, the 10-nm particles seen in sections as well as in properly dried whole mounts are absent. This leads one to suspect that these particles must fuse onto the filaments and contribute to their uneven thickness in the "trabecular" image. I therefore conclude that a pervasive trabecular appearance of cytoplasmic filamentous structure is due to their distortion and fusion with particulate components, most likely the result of surface tension effects due to residual water or ethanol in the CO_2 during CPD.

The structure of cytoplasm as it appears in well-prepared whole mounts is not different from what is seen in thick sections of plastic-embedded cells, except for somewhat greater contrast. In addition to membranous organelles and ribosomes, the cytoplasm contains MT, IF, and actin filaments often interconnected by thinner filaments, the nature of which remains to be elucidated. The absolute and relative amounts of these cytoskeletal elements and the density of cross-connections between themselves and to other cytoplasmic components such as vesicles and ribosomes varies from cell to cell and in different areas of a cell related to cell function. Undoubtedly, many areas of the cytoplasm contained a cross-linked filamentous scaffold, but this is not in the form of a "microtrabecular" lattice formed of tapered strands. It is a lattice formed by distinct filamentous components that make contact with each other and are extensively cross-linked by distinct narrow fibrils. Stereomicrographs of properly dried whole mounts or thick sections obtained by HVEM, combined with studies on living cells as well as biochemical and immunocytochemical approaches should in the future provide information on the molecular nature of the structures involved and the functional significance of

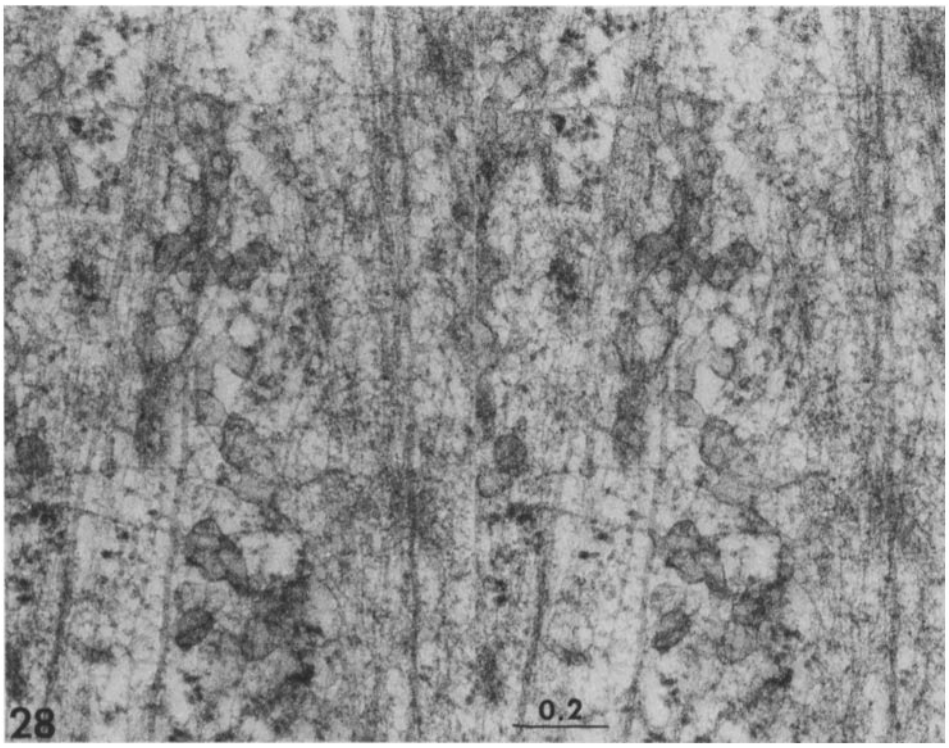

FIGURE 28 BSC-1 cell, section 0.25-μm-thick. Fixation schedule as in WITHOUT TANNIC ACID (a) (glut-HEPES; 1% OsO_4), followed by staining with 1% uranylacetate, and ethanol dehydration, Epon-Araldite. This section shows the complexity of the cytoplasmic filament system including MT, IF, and actin filaments, and cross-links between these elements. All filaments are uniform along their length. Tilt angle 10°. × 60,000.

spatial and temporal variations in the distribution of these various cytoplasmic components.

I wish to thank Ms. Renate Bromberg for expert technical assistance.

This study was supported by a research career program award (K-6-GM21,948). The Madison High Voltage Electron Microscope Facility is supported by a grant from the Biotechnology Resources Program, DRR-NIH (P41RR00570).

Received for publication 4 April 1984, and in revised form 27 December 1984.

REFERENCES

1. Anderson, T. F. 1951. Technique for the preservation of three-dimensional structure in preparing specimens for the electron microscope. *Trans. NY Acad. Sci. (Ser. II)* 13:130–134.
2. Bahr, G. F., and W. F. Engler. 1980. Artifacts observed in critical-point-dried preparations of human chromosomes by electron microscopy. *J. Ultrastr. Res.* 73:27–33.
3. Guatelli, J. C., K. R. Porter, K. L. Anderson, and D. P. Boggs. 1982. Ultrastructure of the cytoplasmic and nuclear matrices of human lymphocytes observed using high voltage electron microscopy of embedment-free sections. *Biol. Cell.* 43:69–80.
4. Maupin-Szamier, P., and T. D. Pollard. 1978. Actin filament destruction by osmium tetroxide. *J. Cell Biol.* 77:837–852.
5. Maupin, P., and T. D. Pollard. 1983. Improved preservation and staining of HeLa cell actin filaments, clathrin-coated membranes, and other cytoplasmic structures by tannic acid-glutaraldehyde-saponin fixation. *J. Cell Biol.* 96:51–62.
6. Otto, J., R. Kane, and J. Bryan. 1979. Formation of filopodia in coelomocytes. *Cell.* 17:285–293.
7. Porter, K. R., and J. B. Tucker. 1981. The ground substance of the living cell. *Sci. Am.* 244:56–67.
8. Ris, H. 1978. Preparation of chromatin and chromosomes for electron microscopy. *Methods in Cell Biol.* 18:229–246.
9. Schliwa, M., and J. van Blerkom. 1981. Structural interaction of cytoskeletal components. *J. Cell Biol.* 90:222–235.
10. Schliwa, M., J. van Blerkom, and K. R. Porter. 1981. Stabilization of the cytoplasmic ground substance in detergent opened cells and a structural and biochemical analysis of its composition. *Proc. Natl. Acad. Sci. USA* 78:4329–4333.
11. Wolosewick, J. J., and K. R. Porter. 1976. Stereo high-voltage electron microscopy of whole cells of the human diploid line, WI-38. *Am. J. Anat.* 147:303–324.
12. Wolosewick, J. J., and K. R. Porter. 1979. Microtrabecular lattice of the cytoplasmic ground substance: artifact or reality. *J. Cell Biol.* 82:114–139.
13. Wolosewick, J. J. 1980. The application of polyethylene glycol (PEG) to electron microscopy. *J. Cell Biol.* 86:675–681.